Tight-Binding Molecular Dynamics with Fermi Operator Expansion: Application to Vacancy Defects in Silicon

Sasfan Arman Wella[a,b], Makoto Nakamura[a], Masao Obata[a], Suprijadi[b], Tatsuki Oda[c]

[a]Graduate School of Natural Science and Technology,
Kanazawa University, Kanazawa 920-1192 Japan,
E-mail: sasfan@cphys.s.kanazawa-u.ac.jp, nakamura@cphys.s.kanazawa-u.ac.jp,
obata@cphys.s.kanazawa-u.ac.jp
[b]Faculty of Mathematics and Natural Sciences, Institut Teknologi Bandung,
Jl. Ganesha 10, Bandung 40132 Indonesia,
E-mail: supri@fi.itb.ac.id
[c]Institute of Science and Engineering, Kanazawa University, Kanazawa 920-1192 Japan,
E-mail: oda@cphys.s.kanazawa-u.ac.jp

Abstract. *By using tight-binding molecular dynamics with Fermi operator expansion, we study vacancy defects in Silicon. The code has been developed for checking silicon crystal, point defect formation energies, etc. The crystal configuration for checking varies among the systems of 64, 216, 512, and 1000 atoms. We have also checked the expansion condition of Fermi operator; the smearing width ($\Delta\varepsilon$), the maximum order of expansion polynomials. The testing shows the good results, compared with the ab initio results. The dynamical behaviors of defects both in the liquid state and the non-self-diffusion state, are still being investigated. In order to support the data analysis, a visualization of multi-vacancy is also constructed.*

Keywords: Fermi expansion, molecular dynamics, tight-binding, vacancy

1 Introduction

Silicon has great economic and technological importance, even nowadays when the limitation of silicon electronic device is claimed. The defects in crystal silicon have been argued and properties of vacancy have interested researchers for a long time in the view point for controlling the defect in electronic devices. In order to investigate silicon defects system, a large system is required. Classical potentials can be applied to large system. However, since they do not treat electronic structure deeply, they are relatively inaccurate when predict many properties. First principle calculations, or *ab initio*, can be quite accurate, but their calculation cost are very high, so that the great computer resources are required. Tight-Binding (TB) method offers a reasonable advantage between these other methods. TB calculation can be faster than first principle calculation and also can handle large system. Compared with classical potentials, TB also gives better accuracy because it treats electronic structure.

In order to investigate dynamical properties of the system, TB method can be applied with molecular dynamics (MD) simulation. Tight-binding molecular dynamics (TBMD) [5, 6] is widely used to investigate dynamical properties of clustering atoms and disordered material and, especially, expected to be able to reveal processes of bond breaking or re-bonding. However, there

are situations where a huge number of time steps in a MD simulation is required. In these cases, even with TBMD simulation, computational time can become a problem if we use standard diagonalization techniques. The present work employed the Fermi operator expansion method [8, 9] which has an order-N property in the computational cost and is suited in massively parallelized computation.

Previously, the TBMD with a Fermi operator expansion (FOE) [11] has been developed and successfully applied to investigate liquid carbon. It will be adapted to investigating defects in silicon system, especially vacancy defects. We also need, however, a potential form. Previous study [10], optimized potential for silicon has been obtained by fitting from experimental reference data and *ab initio* data. This potential describes many properties very accurately and should be useful for this recent work.

2 Tight Binding Molecular Dynamics Model

Adapted from previous study [11], total energy E_{tot} of a crystalline system of nucleus and valence electrons for our TBMD model can be written as

$$E_{\mathrm{tot}} = \sum_i \frac{1}{2} m_i \dot{r}_i^2 + E_{\mathrm{pot}} + \mu \left(N_{\mathrm{ele}} - 2\, \mathrm{Tr}[f(x)] \right), \tag{1}$$

with $E_{\mathrm{pot}} = E_{\mathrm{tb}} + E_{\mathrm{rep}} + E_{\mathrm{ent}}$. First part of equation (1) is total kinetic energy of electrons. Second part is total potential energy, which is represented by three terms of energies: band structure energy E_{tb}, effective repulsive potential E_{rep}, and electronic entropy energy E_{ent}. N_{ele}, μ, and $f(x)$, in the last part, are the number of total valence electron, chemical potential, and Fermi distribution function, respectively. This part is added to satisfy charge neutrality. When the charge neutrality is satisfied, it should be vanish.

To calculate band structure energy E_{tb}, it could be obtained from the sum over all the eigenvalues up to Fermi level with the weight of the Fermi distribution:

$$E_{\mathrm{tb}} = 2 \sum_i \varepsilon_i\, f\left(\frac{\varepsilon_i - \mu}{\Delta\varepsilon} \right), \tag{2}$$

where ε_i is the i-th eigenvalue of the TB Hamiltonian H_{tb} and $\Delta\varepsilon$ is the smearing width of the Fermi level. Equation (2) can also be expressed in terms of trace of H_{tb} with any basis sets:

$$E_{\mathrm{tb}} = 2\, \mathrm{Tr} \left[H_{\mathrm{tb}}\, f\left(\frac{H_{\mathrm{tb}} - \mu}{\Delta\varepsilon} \right) \right]. \tag{3}$$

Using a linear combination of orthogonal atomic orbitals $\{\phi_{l\alpha}\}$, equation (3) can written as

$$E_{\mathrm{tb}} = 2 \sum_{l\,\alpha} \sum_{l'\alpha'} \langle \phi_{l\,\alpha} | H_{\mathrm{tb}} | \phi_{l'\alpha'} \rangle \langle \phi_{l'\alpha'} | f(x) | \phi_{l\,\alpha} \rangle, \tag{4}$$

where, $x = (H_{\mathrm{tb}} - \mu)/\Delta\varepsilon$, l is quantum numbers index and α is label of nuclei.

As shown in equation (4), matrix elements of H_{tb} and $f(x)$ are required to obtain the band structure energy. Construction of H_{tb} for silicon system is different with construction of H_{tb} for carbon system. For silicon system, according to Slater and Koster [4], matrix elements of H_{tb} can be evaluated as two-center integrals. However, potential parameters are required, such as ϵ_{s}, ϵ_{p}, $h_{\mathrm{ss}\sigma}$, $h_{\mathrm{sp}\sigma}$, $h_{\mathrm{pp}\sigma}$, and $h_{\mathrm{pp}\pi}$. According to Lenosky *et al.* [10], these can be obtained by fitting experiment or *ab initio* data. Some data of $g_\alpha = r^2\, h_\alpha$, with $\alpha = ss\sigma, sp\sigma, pp\sigma, pp\pi$, is fitted

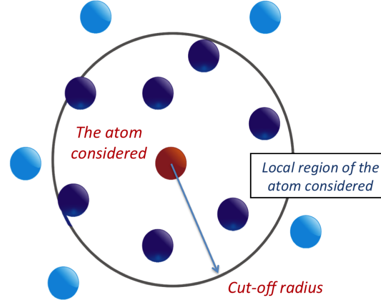

Figure 1: Localization region scheme.

by cubic spline method [1]. These parameters is only fitted for radius range 1.50–5.24 $\mathring{A}$, which is correspond to the first four neighbor shells in the diamond structure. Each matrix element will go smoothly to zero between the third and fourth neighbor shells. For matrix elements of Fermi operator $f(x)$, we can calculate directly by Fermi operator expansion [9, 11], as described in Appendix A.

For electronic entropy energy could be calculated by

$$E_{\mathrm{ent}} = -2\Delta\varepsilon \mathrm{Tr}[s(x)]$$

with

$$s(x) = -\left\{f(x)\ln f(x) + (1 - f(x))\ln(1 - f(x))\right\}.$$

To construct the matrix elements of $s(x)$, we can use the same procedure as for matrix elements of Fermi $f(x)$ with another set of expansion coefficients. And for repulsive energy, it calculated by

$$E_{\mathrm{rep}} = \sum_{i,j} \frac{1}{2}\phi(r_{ij}),$$

where, $\phi(r)$ can be obtained also from previous work [10].

For MD implementation, the equation of motion, which is derived from Lagrangian of the system, can be written as

$$m_i \frac{d^2\mathbf{r}_i}{dt^2} = \mathbf{F}_i = -2\mathrm{Tr}\left[\frac{\mathrm{d}H_{\mathrm{tb}}}{\mathrm{d}\mathbf{r}_i} f(x)\right] - \frac{\mathrm{d}}{\mathrm{d}\mathbf{r}_i} E_{\mathrm{rep}}. \tag{5}$$

Equation of motion as shown in equation (5) is integrated with Verlet algorithm to update the position and velocity of atoms. During we calculate the force, a localization region (LR) are introduced, which is associated with each atom. The number of atom will be determined by cut-off radius r_{cutoff} of the region (see Figure 1). This feature allow us to reduce the number of Tight-Binding bases without lossing the accuracy of the calculations. This feature also allow us to parallelize the calculation because force calculation for each atom is totally independent.

3 Result and Discussion

Before investigating the silicon system, because of LR is used, the best cut-off radius $r_{\rm cutoff}$ should be chosen to optimize the calculation. Cut-off radius $r_{\rm cutoff}$ related with the number of atoms, and number of atoms related with accuracy and time of the calculations. For $4 \times 4 \times 4$ silicon system, cut-off radius $r_{\rm cutoff}$ should be chosen in range $0.85 - 1.1$ nm, because point defect energies are saturated (see Figure 2). In this range, point defect energy for each $r_{\rm cutoff}$ quite similar, but time of calculation is different. Time cost can be saved by choosing the best cut-off radius.

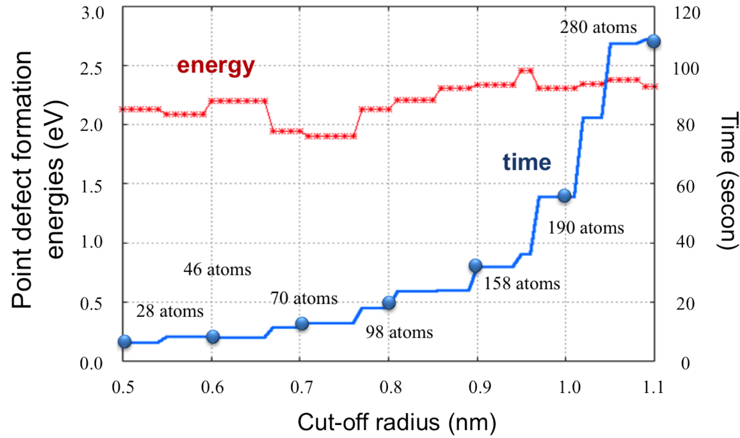

Figure 2: Dependence of cut-off radius $r_{\rm cutoff}$ to accuracy and time of calculation.

In this investigation, we determine point defect formation energy. Point defect formation energy is important to know the stability of the system while the complete system losses some atom. From previous study [2], point defect formation energy is written by

$$E_f = E_{\rm vacancy} - \left(\frac{N-1}{N}\right) E_{\rm bulk} + q\mu, \tag{6}$$

where, E_f is point defect formation energy, $E_{\rm vacancy}$ is total energy of vacancy defect system, $E_{\rm bulk}$ is total energy of complete system, q is charge, and μ is chemical potential. We use equation (6) to determine point defect formation energy for several smearing ($\Delta\varepsilon$). Because of charge neutrality, the last part should be neglected. Figure 3 showed us point defect formation energy for several smearing ($\Delta\varepsilon$) and also for several size of silicon system: $2 \times 2 \times 2$ (64 atoms), $3 \times 3 \times 3$ (216 atoms), $4 \times 4 \times 4$ (512 atoms), and $5 \times 5 \times 5$ (1000 atoms). When larger smearing is used, we will get smaller point defect formation energy compare with calculation with small smearing. This case comes from electronic entropy energy, because when smearing is increase (temperature increase), possibility to find electrons above Fermi level is also increase. To calculate point defect formation energy with small smearing, high accuration is required. Degree of polynomial ($n_{\rm pl}$) should be increase to handle that situation.

In zero temperature case ($\Delta\varepsilon = 0$), point defect formation energy is calculated in unrelaxed and relaxed defect configuration. Compare with previous models [10, 3] and *ab initio* result [7], our model show good results (see Table 1 and Tabel 2).

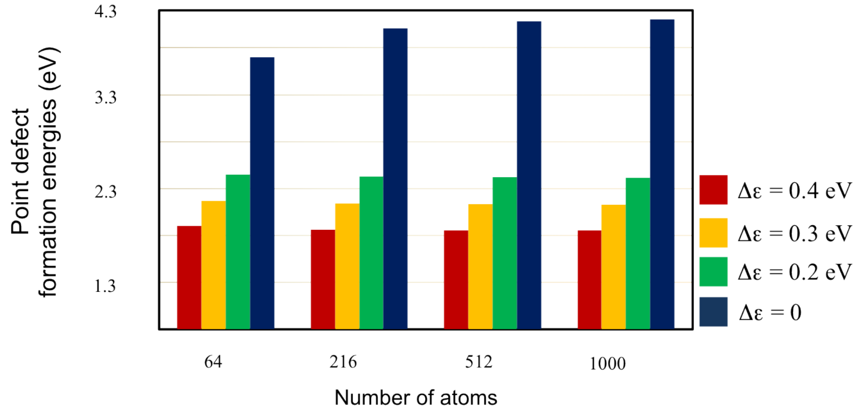

Figure 3: Point defect formation energy for several smearing ($\Delta\varepsilon$).

Table 1: Point defect formation energies (in eV) in unrelaxed defect configuration.

Our model				Lenosky *et al.* [10]		Kwon *et al.* [3]		*Ab initio* [7]
64	216	512	1000	64	216	64	216	
3.645	3.989	4.076	4.102	3.639	3.984	4.720	5.570	4.400

Table 2: Point defect formation energies (in eV) in relaxed defect configuration.

Our model				Lenosky *et al.* [10]		Kwon *et al.* [3]		*Ab initio* [7]
64	216	512	1000	64	216	64	216	
3.505	3.801	3.897	4.102	3.949	3.397	3.780	3.390	3.600

We also interest to consider the dynamical behaviors of defects both in the liquid state and the non-self-diffusion state. First we use $5 \times 5 \times 5$ (1000 atoms) silicon system and then 10 atoms is removed from this system. In the other hand, we have multi-vacancy system with 990 atoms. Temperature above melting point is chosen when consider behavior of defects in the liquid state, and temperature below the melting point for non-self-diffusion state. In order to support the data analysis, a visualization of multi-vacancy is also constructed. In the real system with vacancy defects, defects are represented by holes. In order to consider the dynamical behavior of defects, we should reprensent the hole with a visualization form. Test points are used to visualize the hole. First we put test points so that fulfill the superlattice (see Figure 4(a)) and then make the selection (see Figure 4(b)). This selection method is quite similar with localization region. In this part, we choose a cut-off range associated with each test point. If silicon atom is exist inside the region, the test point will be removed, otherwise will be kept.

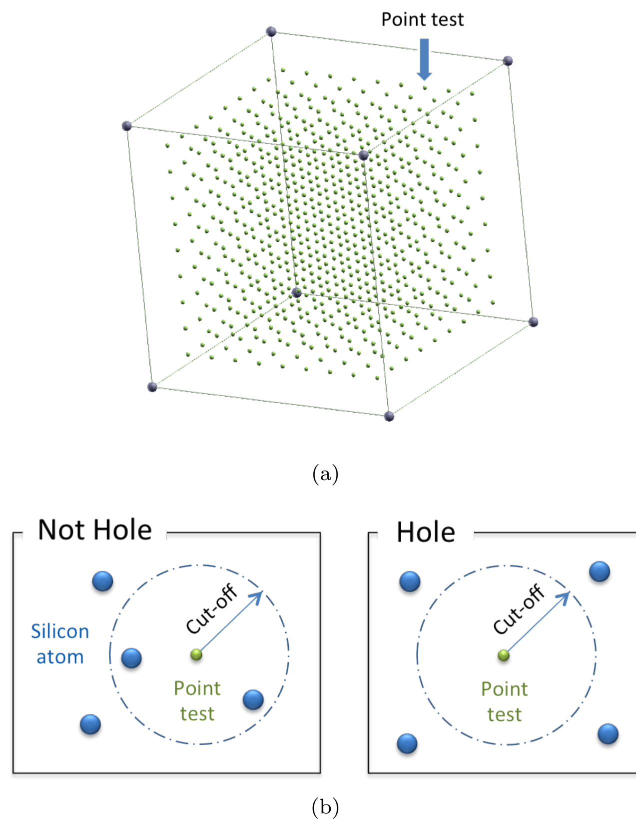

Figure 4: (a) Test points configuration, (b) Test points selection scheme.

Using this method, we can consider the dynamical behaviors of defects quite easily. As shown in Figure 5, for liquid state case, the hole will be disappear because atoms near hole will be diffused to fill the hole. For non-self-diffusion case (see Figure 6), the hole looks vibration. In our opinion, long time simulation will has possibility to find the movement of the hole. Checking the energy convergence is required to satisfy the calculation. From Figure 7(a) and Figure 7(b), we can see the temperature control by Nose termostat has worked properly, and from Figure 8(a) and Figure

8(b), we can see both in liquid state case and non-self-diffusion case, total energies are convergen.

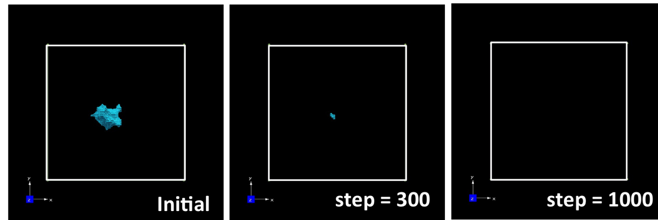

Figure 5: Dynamical behavior of defects in liquid state (1700 K).

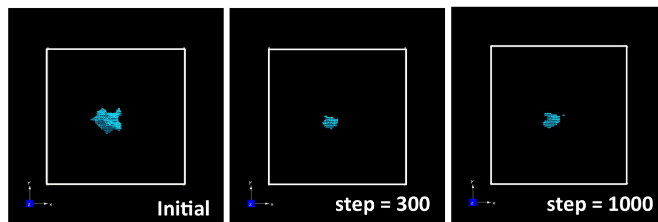

Figure 6: Dynamical behavior of defects in non-self-diffusion (1100 K).

4 Summary

TMBD with FEO has been applied to crystal silicon system (with defects) and the results (point defect formation energies) show the value comparable to *ab initio* result and other previous works. For Condition of Fermi operator also has been checked. Better result has been obtained, especially when we consider zero temperature case. In this case, however, high degree of polynomial is required to increase the accuracy. To consider behaviors of the defects in multi-vacancy system, a visualization has been constructed. The movement of the hole will be possible to found in non-self-diffusion with long time calculation. For liquid state case, the hole will be disappear because atoms near the hole will be diffuse to fill the hole.

Acknowledgment

The authors would like to JASSO (Japan Student Services Organization) and Beasiswa Unggulan DIKTI (Ministry of Education and Culture of Indonesia) for finansial support of this research.

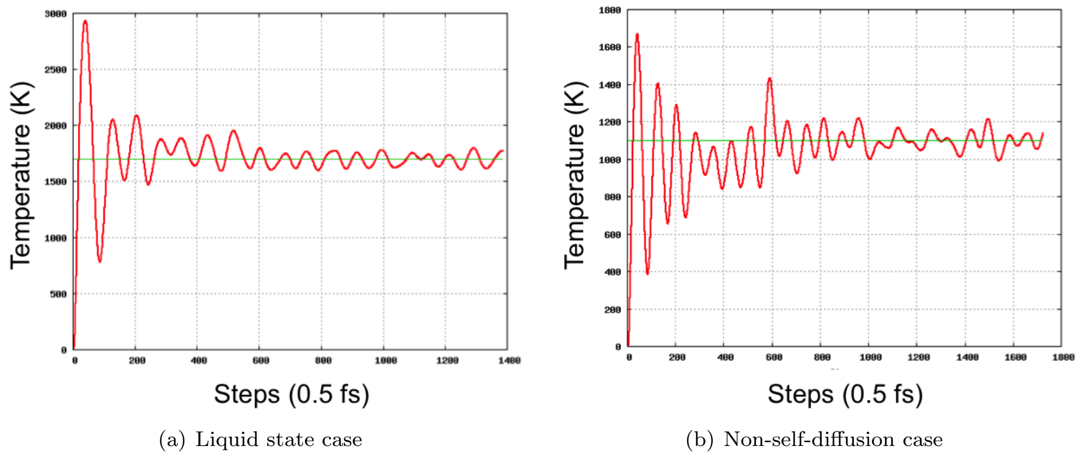

(a) Liquid state case (b) Non-self-diffusion case

Figure 7: Time evolution of temperature system.

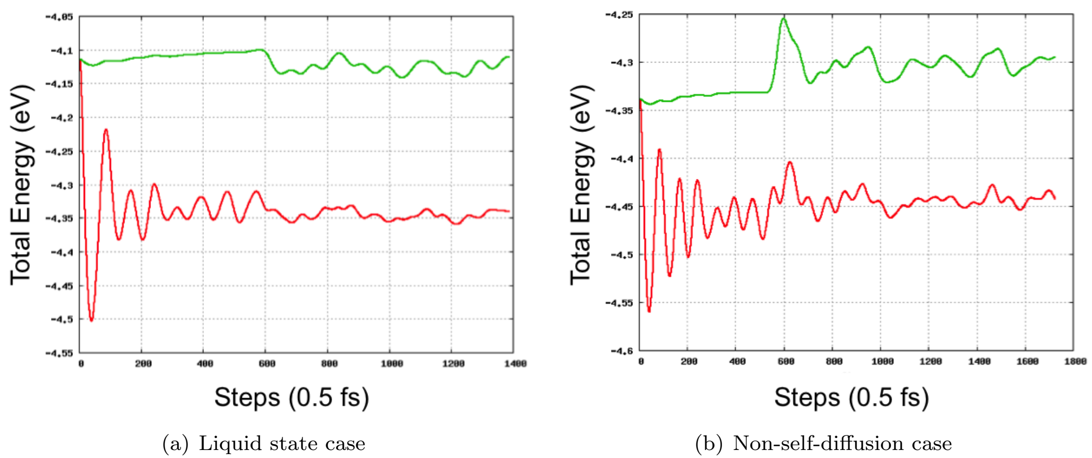

(a) Liquid state case (b) Non-self-diffusion case

Figure 8: Time evolution of total energy system.

References

[1] A. L. Burden and J. D. Faires (2010). *Numerical Analysis, Ninth Edition.* Rooks-Cole, Cengage Learning, Boston.

[2] F. Corsetti and A. A. Mostofi (2011). System-size convergence of point defect properties: The case of the silicon vacancy. *Phys. Rev. B*, **84**, 035209.

[3] I. Kwon *et al.* (1994). Transferable tight-binding models for silicon. *Phys. Rev. B*, **49**, 7242–7250.

[4] J. C. Slater and G. F. Koster (1954). Simplified LCAO Method for the Periodic Potential Problem. *Phys. Rev.*, **94**, 1498–1524.

[5] L. Goodwin, A. J. Skinner, and D. G. Pettifor (1989). Generating transferable tight-binding parameters: application to silicon. *Europhys. Lett.*, **9**, 701.

[6] L. Goodwin (1991). A new tight binding parameterization for carbon. *J. Phys. Condens. Matter*, **3**, 3869.

[7] P. J. Kelly and R. Car (1992). Greens-matrix calculation of total energies of point defects in silicon. *Phys. Rev. B*, **45**, 6543–6563.

[8] S. Goedecker and L. Colombo (1994). Efficient linear scaling algorithm for tight-binding molecular dynamics. *Phys. Rev. Lett.*, **73**, 122–125.

[9] S. Goedecker and M. Teter (1995). Tight-binding electronic-structure calculations and tight-binding with localized orbital. *Phys. Rev. B*, **51**, 9455–9464.

[10] T. J. Lenosky *et al.* (1997). Highly optimized tight-binding model of silicon. *Phys. Rev. B*, **55**, 1528–1544.

[11] T. Oda and Y. Hiwatari (2000). Order-N tight-binding molecular dynamics simulation with a Fermi operator expansion approach: application to a liquid carbon. *J. Phys. Condens. Matter*, **12**, 1627–1639.

Appendix A : Fermi Operator Expansion

Fermi distribution function is expanded by Chebyshev as following equation

$$f(x) \approx p(t) = \frac{c_0}{2} + \sum_{j=1}^{n_{\mathrm{pl}}} c_j \, T_j(t). \tag{7}$$

We need to rescale t from x with this relation:

$$x = \frac{x_{\max} - x_{\min}}{2} t + \frac{1}{2}(x_{\max} + x_{\min}),$$

where, $x_{\max}$ and $x_{\min}$ are the maximum and the minimum eigenvalues of x, respectively. With this scaling, the eigenvalues of t should be in the range between -1 and 1. The degree of polynomial in equation (7), can be chosen by following relation:

$$n_{\mathrm{pl}} = C \frac{W}{\Delta\varepsilon}$$

where $W \sim 2\Delta\varepsilon \max(x_{\max}, |x_{\min}|)$ represent a bandwidth of the electronic structure, and C is a constant. For expansion coefficients, it can be obtained by this following formula:

$$c_j = \frac{2}{\pi} \int_{-1}^{1} f[p] T_j(p) \frac{\mathrm{d}p}{\sqrt{1-p^2}}. \tag{8}$$

Practically, however, we used $x_{\min} = -x_{\max}$ and the expansion coefficients can be obtained by

$$c_j = \begin{cases} 1 & \text{for } j = 0 \\ \frac{4}{\pi} \int_0^{p_1} \left(f[p] - \frac{1}{2} \right) T_j(p) \frac{\mathrm{d}p}{\sqrt{1-p^2}} - \frac{4}{\pi} \frac{\sin(j\theta_1)}{2j} & \text{for } j = \text{odd} \\ 0 & \text{otherwise} \end{cases}$$

where $p_1 = \cos\theta_1$ with $0 \leq \theta_1 \leq \pi/2$.